Quantification of relaxor behavior in (1 – x)Na0.5Bi0.5TiO3 – xCaTiO3 lead-free ceramics system

Roy Roukos, Jimmy Romanos, Sara Abou Dargham, Denis Chaumont

Version of Record: https://www.sciencedirect.com/science/article/pii/S0955221919300986
Manuscript_2aad471c9402ef3d86b65e005eeaf3c1

Quantification of Relaxor Behavior in (1-x)$Na_{0.5}Bi_{0.5}TiO_3$ – x$CaTiO_3$ Lead-free Ceramics System

Roy Roukos[a,*], Jimmy Romanos[b], Sara Abou Dargham[b], Denis Chaumont[a]

[a] *Laboratoire Interdisciplinaire Carnot de Bourgogne UMR 6303 CNRS, Université de Bourgogne, 9 Avenue Alain Savary, Dijon, 21078, France*
[b] *Department of Natural Sciences, Lebanese American University, Byblos, P.O.Box 36, Lebanon*

Abstract

This work examines the relaxor behavior of lead-free ceramic (1-x)$Na_{0.5}Bi_{0.5}TiO_3$–x$CaTiO_3$ systems. A stable rhombohedral *(R3c)* phase is detected at room temperature for all compositions by XRD and Raman spectroscopy. Relaxor behavior was observed in the temperature range 300 K - 400 K for all materials. Ceramics exhibit normal ferroelectric properties at room temperature, and then they develop relaxor characteristics with increasing temperature showing the same dispersive properties. This work quantifies the relaxor phenomenon at low temperature. For instance, the maximum temperature of relaxor and the order of dispersion were determined at the strongest dispersion. Finally, the substitution by low CT concentration unaltered the relaxor behavior at low temperature.

Keywords: NBT-CT, Dielectric properties, Relaxor behavior, Order of dispersion

1. Introduction

$Na_{0.5}Bi_{0.5}TiO_3$ (NBT) is considered among promising lead-free relaxor materials and a potential candidate to replace lead-relaxor materials such as $Pb(Mg_{1/3}Nb_{2/3})O_3$. NBT has been widely studied in recent years due to its structural varieties [1–3] as well as its interesting dielectric, piezoelectric and electromechanical properties [4–6]. At ambient temperature, NBT is rhombohedral with polar space group *(R3c)* [1, 7]. Recently, several works reported that the structure of this material is a stable monoclinic phase *(Cc)* at room temperature [8, 9].

Extensive studies of this based material showed at least two successive sequences of phase transitions as a function of temperature using XRD, neutrons, as well as Raman spectroscopy [1, 10–12]. Upon heating, the rhombohedral *(R3c)* phase is transformed into an intermediate tetragonal *(P4bm)* symmetry around 150 °C (423 K). These two phases seem to coexist simultaneously between 250-400 °C (523-673 K) [1, 13, 14], making NBT an unusual system with a specific behavior. Previous studies have shown that the *R3c* –

*Corresponding author.
Email address: roy.roukos@gmail.com (Roy Roukos)

P4bm transition takes place around 300 °C (573 K) or 320 °C (593 K) with a diffuse phase transition (DPT) [11, 14, 15]. Otherwise, the transition from tetragonal *(P4bm)* to cubic *(Pm3m)* occurs above 520-540 °C (793-813 K) [1, 16]. Recently, Raman spectroscopy showed that the two phases (tetragonal and cubic) coexist around 500 °C (773 K) just before the complete transition to the centrosymmetric structure [14].

NBT is ferroelectric at room temperature. However, the dielectric properties at different temperatures are still under investigation due to the lack of correlation between dielectric anomalies and structural properties. The temperature dependence of the dielectric permittivity exhibits two anomalies. The first anomaly, occurring at 200 °C (473 K), is attributed to ferroelectric – antiferroelectric phase transition [11, 17–19], which corresponds to the depolarization temperature (T_d). This anomaly appears as a strong frequency-dependent shoulder, extending over a temperature range from 200 °C (473 K) to 250 °C (523 K) [20].This corresponds to a relaxor behavior and marks the end of the ferroelectric state of the material. The second transition, occurring around 320 °C (593 K), is associated with a transition from antiferroelectric to paraelectric phase [11, 14, 17].

Recent literature focused on studying the frequency dispersion observed at low temperature. The obtained results defined this anomaly as a transition from ferroelectric to relaxor state (F–R) [21, 22] without involving any phase transition such as ferroelectric – antiferroelectric state (T_d). The determination of this transition temperature (T_{F-R}) is only valid for poled samples from the dielectric loss ($\tan\delta$) [23, 24].

Classified as a relaxor ferroelectric, the A-site of NBT-based system is occupied randomly by Na^+ and Bi^{3+} which is exceptional for the most ABO_3 system. For this reason, the origin of the relaxor behavior obtained at low temperature is still unclear. Consequently, there are many reports from different research groups trying to establish a relationship between the structure, the dielectric properties, and its relaxor behavior [15, 25, 26]. Tu et al. [25] reported the existence of superparaelectric micropolar clusters responsible for relaxor phenomenon. Whereas, Perk et al. [27] proposed a change in the size and the dynamics of polar regions. The XRD analysis of NBT reported by Suchanicz et al. [12] showed the coexistence of rhombohedral and tetragonal phases over a wide temperature range. In addition, the dielectric properties of NBT highlighted the existence of polar regions [28]. Furthermore, Vakhrushev et al. [13] proved that these polar regions are unstable. Moreover, the ^{23}Na NMR spectra of NBT between 123-447 °C (396-720 K) showed that the material contains regions with polar clusters distributed in cubic matrix [29]. Afterwards, in situ TEM studies by Dorcet et al. [12, 15] showed that the rhombohedral *(R3c)* structure of NBT transforms into a modulated orthorhombic *(Pnma)* structure. This modulated phase is grown as orthorhombic sheets in a rhombohedral matrix or blocks at 200 °C (473 K). This result is believed to be responsible of the relaxor behavior. Recently, Barick et al. indicated that the NBT is considered as a relaxor due to the disorder at A-site and the dielectric relaxation is "non-Debye" type [11].

An interesting feature of NBT-based material is its ability to form solid solutions by substitution at A-site and/or B-site. In order to understand the relaxor behavior and to develop lead-free relaxor for high temperature applications, several binary NBT-based solid solutions with other perovskites have been studied [30, 31]. The famous solid solutions

display a strong relaxor behavior at high value of substitution with ST ($SrTiO_3$) [14, 32, 33]. The origin of the relaxor is attributed to formation of the micropolar regions in this system [34]. Moreover, Roukos et al. [35] showed a similar relaxor behavior with CT-dopant ($CaTiO_3$) where its concentration is very high and exceeds $x \geq 0.15$.

More recent investigations of the phase stability of the relaxor revealed that the electric field induced phase transition and allowed to obtain relaxor properties in the NBT – BT ($BaTiO_3$) ferroelectric system [23, 36]. This was explained by the formation of polar nanoregions (PNRs) of different symmetries. In light of these new results, it is important to consider the correlation between the structure and the dielectric properties of these materials.

While most research in the field focuses on qualitative structural and dielectric properties of lead-free materials, this manuscript study the quantification of the relaxor phenomenon at low temperature. Most studies of Ca-modified NBT reported on the stuctural characteristics exclusively [37–39]. In light of the unique properties shown by this system, this paper reports detailed structural analysis, vibrational analysis and dielectric properties of (1-x)NBT – xCT system. A relaxor behavior is reported at low temperature independently of x for all compositions. We introduce a new concept, order of dispersion, to quantify and explain this phenomenon. This concept allows to determine the maximum temperature of relaxor (T_{MR}) for high dispersion.

2. Methods

Powder and ceramic samples of (1-x)NBT – xCT (x = 0.00, 0.01, 0.05 and 0.07) were prepared by a solid oxide route using reagent-grade powders of Na_2CO_3 (Prolabo), $CaCO_3$ (Alfa Aesar), Bi_2O_3 (Alfa Aesar), and TiO_2 (Alfa Aesar) (purity greater than 99.6%). A stoichiometric amount of these powders were mixed, milled and calcined twice at 750 °C and 950 °C for 4 hours. After this, powders were pressed into pellets with a 13 mm diameter and sintered at 1075 °C for 1 hour in a confined environment. The ceramics densities were measured with the Archimedes method using distilled water. The densities obtained are between 96 – 97%.

The crystalline structure was examined by X-ray diffraction (XRD) using a D8 advance X-ray diffractometer (Vantec detector) with CuKα radiations (λ = 1.5405 Å) in the 2θ range of 20° - 90°. The data were reported with a step size of 0.017 and a scanning time of 10 s. Raman spectra were recorded between 4 and 700 cm^{-1} at room temperature using Jobin-Yvon T64000 spectrometer HR (high resolution) equipped with Ar-ion laser operated at 514.5 nm and adjusted at 20 mW for excitation with liquid N_2-cooled system couple device detector. The dielectric properties were measured with bulk ceramics coated with gold electrodes for low temperature characterization. The dielectric measurements were performed using an HP-4284A LCR meter in the temperature range of 70 – 450 K at various frequencies (100 Hz - 1 MHz).

3. Results and Discussion

3.1. Structural and vibrational properties of (1-x)NBT – xCT systems

(1-x)NBT – xCT with $0.00 \leq x \leq 0.07$ solid solutions are single phase pure perovskite ABO_3 structure at room temperature as shown in the XRD patterns of Figure 1(a). No traces of secondary phase were detected. The rhombohedral characteristic peaks were clearly identified. An expanded view of the XRD in the 2θ region between 36 and 50° shows the superlattice reflection $(113)_R$ characteristic of the rhombohedral phase with *(R3c)* as space group for all compositions, as displayed in Figure 1(b). This implies that the Ca^{2+} was completely diffused and well substituted into the A-sites of NBT in order to form NBT - CT solid solutions. Recent Rietvield refinement studies showed that NBT exhibits a monoclinic phase *(Cc)* instead the rhombohedral *(R3c)* [8]. Effectively, many attempts were carried out by Rietveld refinement with the monoclinic *(Cc)* phase and the obtained results did not permit describing the structure in our system. The structure is refined to a rhombohedral cell and the good quality of fit is obtained with *(R3c)* model (Figure 1(c)) since the difference between the theoretical and experimental peaks is relatively small. The inset in (Figure 1(c)) shows a magnified plot of $(110)_R$ and $(024)_R$ confirming the quality of the Rietveld refinement and highlights the proposed *R3c* model.

Raman spectroscopy, considered sensitive to phase transitions in these materials, was used to complement the XRD results. Raman spectra of (1-x)NBT – xCT ($0 \leq x \leq 0.07$) solid solutions at room temperature are displayed in Figure 2. The main bands of NBT are detected in the wavenumber range 4 – 700 cm^{-1} which is very similar to that reported previously on other NBT-based ceramics [12, 14, 40]. Broad bands and overlapping Raman modes in (1-x)NBT – xCT spectra are caused by the A-site (Na/Bi and Ca) disorder.

Four characteristic Raman modes can be observed in this wavenumber range. The first two modes are attributed to the Bi-O (25 cm^{-1}) and Na-O (138 cm^{-1}) bands of the A-site vibration in the perovskite structure, while the third peak situated at 286 cm^{-1} is associated with the Ti-O vibration mode. The modes at 530 cm^{-1} and 584 cm^{-1} correspond to the TiO_6 octahedral vibrations. Note that, for all compositions, there are no band shifting or splitting with increasing x. This indicates that the symmetry was conserved since no change in the Raman-active modes were detected. In fact, this behavior demonstrates that these materials maintain their symmetry similar to NBT-based system and exhibit a rhombohedral phase *(R3c)* as reported in XRD analysis (Figure 1). The A-site substitution of NBT does not induce variations in the Raman spectra and XRD patterns, this could be attributed to the low concentration of CT used in this study.

The dependence of the microstructure on CT concentration was studied using scanning electron microscopy (SEM) on a JEOL 7600F. The SEM micrographs (provided in the supplementary information) shows that the microstructure consists of uniform grain size with high densification. No noticeable difference in terms of morphology and grain size was detected by increasing CT concentration. In contrast to other studies performed with Sr^{2+} [33], the addition of Ca^{2+} does not have an impact on the microstructure.

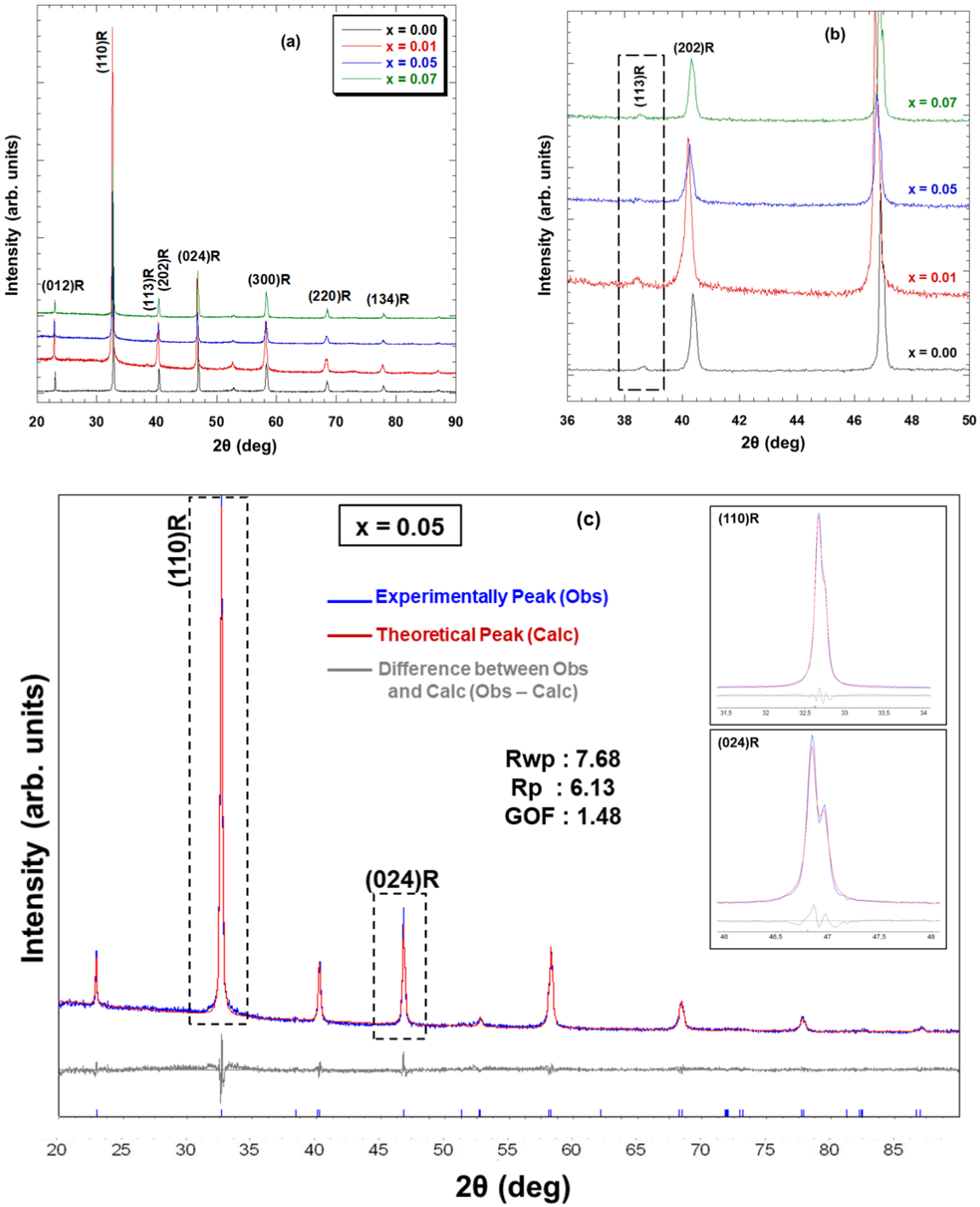

Figure 1: (a)XRD patterns of (1-x)NBT – xCT / ($0.00 \leq x \leq 0.07$) solid solutions at room temperature; (b) Enlarged view of the 2θ between 36 – 50° showing the superlattice reflection $(113)_R$ features of the rhombohedral phase for all compositions (in rectangle); (c) An example of the Rietveld refinement of the XRD pattern for x = 0.05 solid solution. The red solid line represents the obtained diffraction pattern and the blue solid line shows the calculated fit. The diffraction of the *R3c* is exhibited as vertical lines with the difference between the theoretical and experimental above. The quality of fit (Rwp, Rp, GOF) is reported besides proving the good agreement of the *(R3c)* model. The inset displays experimental peaks of $(110)_R$ and $(024)_R$ alongside the peaks calculated by Rietveld refinement for x=0.05.

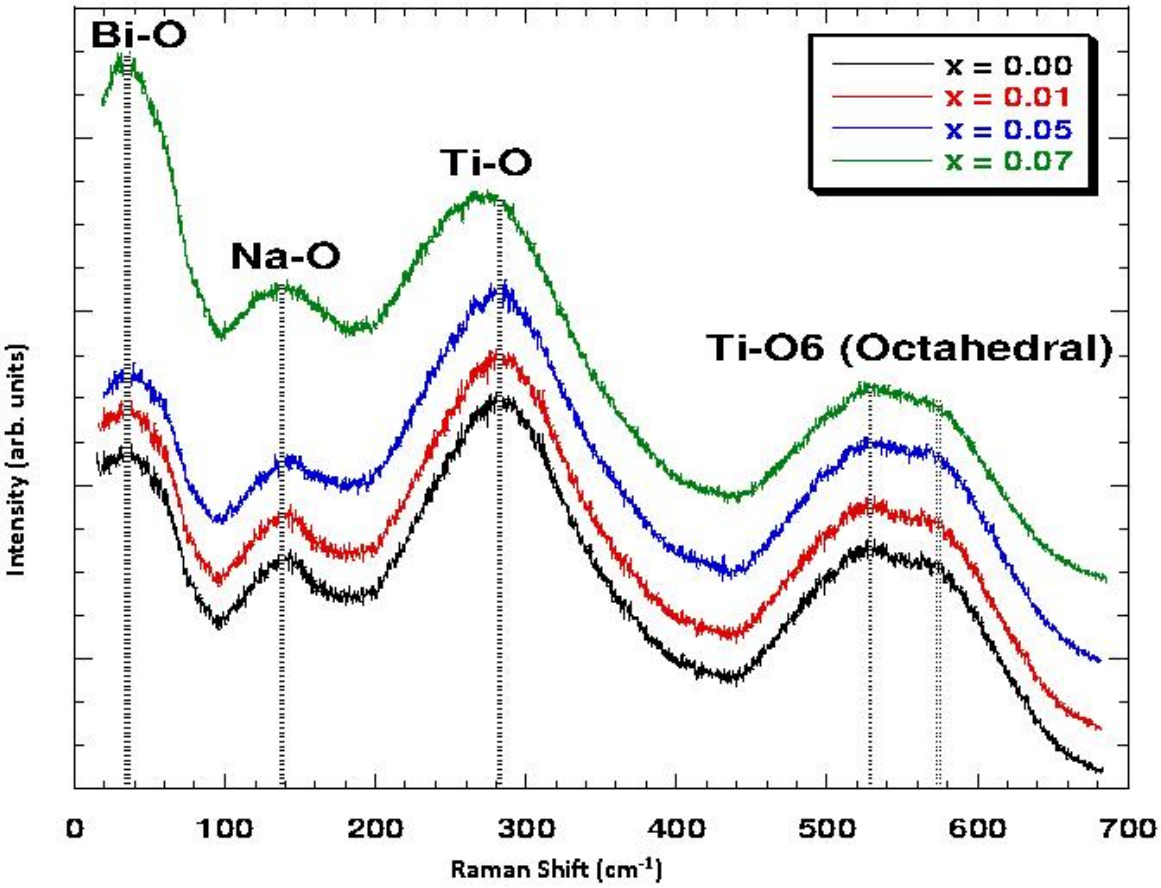

Figure 2: Raman spectra of (1-x)NBT – xCT solid solutions with different CT concentrations ($0 \leq x \leq 0.07$) at room temperature.

3.2. Dielectric behavior of (1-x)NBT – xCT ceramics at low temperature

The evolution of the complex dielectric permittivity (ε and $\tan\delta$) at low temperature range (70 – 450 K) as a function of x at different frequencies is shown in Figure 3. The results indicate that the behavior of the permittivity for all ceramics is similar independently of the percentage of Ca^{2+} dopant. By analogy with the pure NBT (x = 0.00), the same dielectric anomaly was observed in this temperature range when $x \leq 0.07$. All these ceramics show an anomaly as a shoulder around 440 K (T_{F-R}). This anomaly, explained by a relaxor behavior due to the frequency dispersion [24, 36], appears clearly in the dielectric loss ($\tan\delta$) and is associated with the transition from ferroelectric to relaxor state [21, 22]. Unlike typical relaxors, the permittivity continues to rise as the temperature increases. This behavior appears for the solid solutions containing low concentration of CT whose rhombohedral symmetry is established. For $x \geq 0.15$, the shoulder disappears reflecting the absence of similar anomaly when solid solutions crystallize in an orthorhombic phase [35, 41]. A typical relaxor is obtained for this substitution which widely established for ABO_3 ferroelectric

perovskite [34, 42].

Recent studies showed that the anomaly, which appears at low temperature, is observed in materials having a stable phase relaxor with coexistence of polar nanoregions (PNRs) with different symmetries (rhombohedral + tetragonal). This is only observed in NBT-based relaxor ferroelectrics, such as NBT-BT [21], NBT-KBT-ST [43], and NBT-BT-BZT [36] systems. In our case, for $0 \leq x \leq 0.07$, the dielectric anomaly obtained at low temperature is due to the thermal evolution of rhombohedral PNRs leading to the transition ferroelectric – relaxor state.

This anomaly was previously called depolarization temperature T_d, a name that is traditionally attributed to a transition between the ferroelectric phase and antiferroelectric phase [11, 17, 25]. Note that there are several contradictory explanations on T_d. However, most studies consider it an intermediate state related to ferroelectric – antiferroelectric phase transition [44]. This is accompanied by a structural change resulting in the instability of the rhombohedral phase *(R3c)* which gradually transform into the tetragonal phase *(P4bm)* distributed randomly within the *R3c* matrix. The mixture of these two phases generates the relaxor behavior. In fact, for $x \leq 0.07$, the evolution of the $\varepsilon'(T)$ exhibits a frequency dispersion appearing as a shoulder which corresponds to a maximum on the dielectric loss ($\tan\delta_m$ at 400 K). These results are in agreement with those previously reported and the corresponding temperatures are about the same as those found for NBT [14, 45].

In contrast to other studies [46, 47], the temperature T_{F-R} remains almost unchanged; it is practically independent of the substitution for $x \leq 0.07$. It was demonstrated that only T_m (maximum temperature related to the antiferroelectric/paraelectric transition) is obtained at high temperature and moves towards the lower temperature when x increases. This is supported by Raman spectroscopy and DSC measurement [41]. For instance, T_m shifts towards T_{F-R} so that the difference between these two temperatures decreases as x increases. This suggests that the phase transition is enhanced at low temperature with CT dopant.

3.3. Study and Quantification of relaxor phenomenon

Based on the observed frequency-dependent broad shoulder for all ceramics, an expression has been reported to better characterize this dispersion and to determine its maximum. This dimensionless magnitude, called amplitude of dispersion, analyzes the relation between frequency and the evolution of the real part of the permittivity (ε').

Several temperatures were chosen over the entire range of measurement frequencies. For each temperature, the corresponding value of the permittivity (ε') has been determined. Then, these values are normalized versus ε'(100 Hz) according to the following formula:

$$\varepsilon'_{N(x,f)} = \frac{\varepsilon'_{(x,f)}}{\varepsilon'_{(x,100\ Hz)}} \tag{1}$$

where $\varepsilon'_{N(x,f)}$ represents the normalized real part of the permittivity, at the frequency f and for a doping concentration x; $\varepsilon'_{(x,f)}$is the measured real part of the permittivity, at the frequency f and for a doping concentration x; $\varepsilon'_{(x,100\ Hz)}$ is the measured real part of the permittivity, at the frequency 100 Hz and for a doping concentration x.

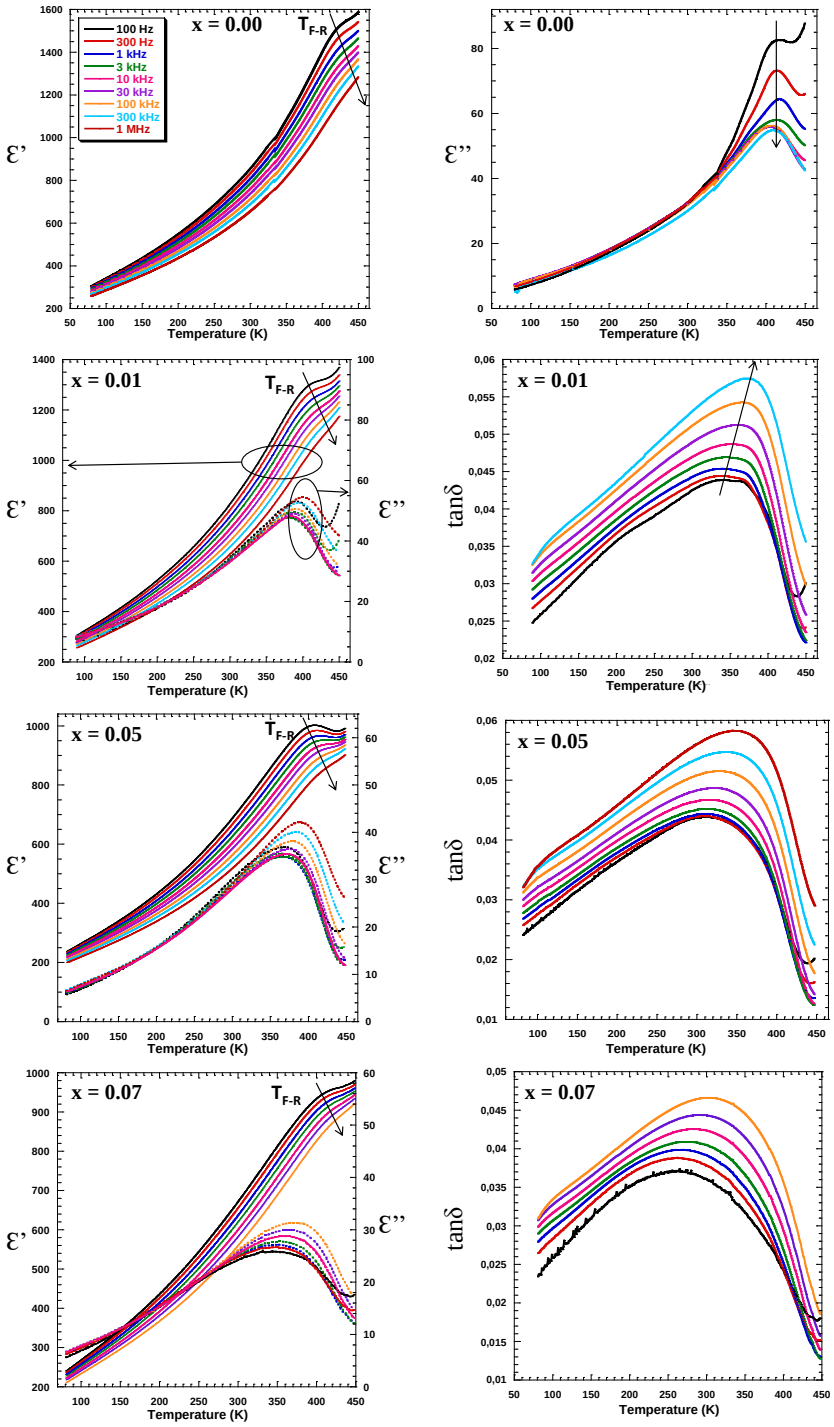

Figure 3: Dielectric permittivities (Real part ε', imaginary part ε", loss tanδ) versus temperature, measured on (1-x)NBT– xCT ($0 \leq x \leq 0.07$) ceramics at different frequencies (100 Hz – 1 MHz).

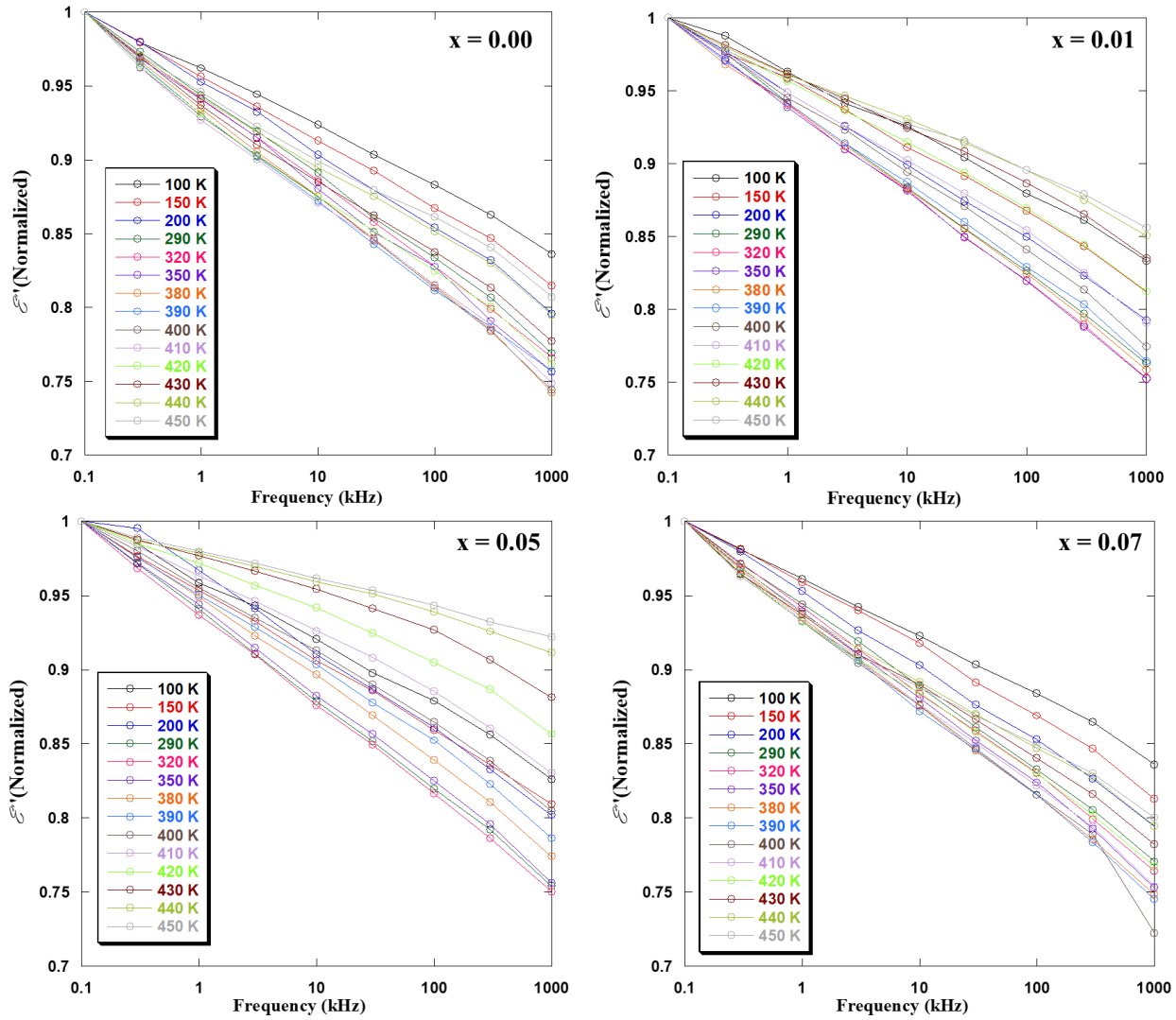

Figure 4: Evolution of the normalized real part of the permittivity for all compositions of (1-x)NBT – xCT ceramics (x = 0, 0.01, 0.05 and 0.07) as a function of frequency at different temperature.

The normalized values were plotted as a function of the measurement frequency (Figure 4). The obtained curves are linear decreasing as a function of the frequency. Afterwards, these curves are fitted by a power function ax^b (supplementary information). The absolute values of b determine the dispersion magnitude and the amplitude for each temperature. Then, it is plotted as a function of temperature (Figure 5). This allows to identify and quantify the dispersive nature of the material. This procedure is applied to all ceramics x = 0.00, 0.01, 0.05 and 0.07. Figure 5 shows the variation of the order of dispersion magnitude relative to the different compositions of ceramics as a function of temperature. At low temperature, they exhibit a weak dispersion and then, upon heating, it becomes more remarkable around T_{F-R}. The dispersion reaches a maximum around a defined temperature

called maximum relaxor temperature (T_{MR}). This is followed by a sharp decrease and then, the dispersion disappears at high temperatures for all compositions in order to join the second anomaly (T_m) which is frequency-independent. This is in accordance with the dielectric properties at high temperature [41]. The same behavior is observed for all ceramics (x = 0.01, 0.05 and 0.07). Consequently, the same dispersive behavior is clearly observed in these compositions.

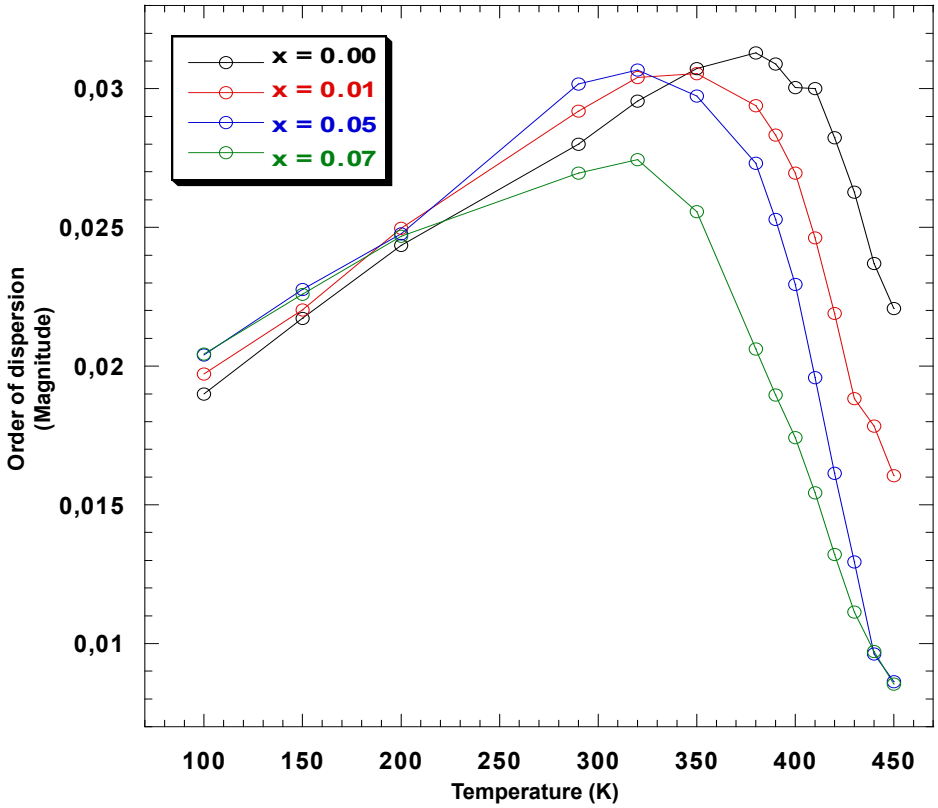

Figure 5: Evolution of the dielectric dispersion amplitude (magnitude) as a function of temperature for (1-x)NBT – xCT system / x = 0.00, 0.01, 0.05 and 0.07.

By analogy to other systems, a similar relaxor behavior is obtained for NBT-based solid solution such as NBT-BT [23], where the materials undergo a phase transition from ferroelectric to relaxor phase under poled conditions. Although, the structure is rhombohedral *(R3c)* in this study, the dielectric behavior of these samples is also similar to systems near the MPB compositions. This feature is validated for x = 0.07 where it is located near the MPB composition for the (1-x)NBT – xCT system [41]. In our case, the relaxor behavior is due to the existence of polar nanoregions (PNRs nano-domains). At this instant, upon heating, the ferroelectric long range order phase breaks up and then, the materials transform

into short range ordered state. These formed PNRs gives rise to the obtained frequency dispersion at the T_{F-R}.

Evidence of polar nanoregions were shown by TEM [21, 48]. The reported results in refernce [21] revealed a nanoscale dimension of rhombohedral *(R3c)* and tetragonal *(P4bm)* symmetries indicated by the presence of the superlattice reflections $\frac{1}{2}$(ooo) and $\frac{1}{2}$(ooe) respectively. In addition, these nanodomains did not show any splitting in XRD analysis [23]. In analogy with our XRD patterns (Figure 1), we found out that there is no additional peak or splitting affecting these ceramics. Furthermore, the TEM bright field images reported by Ma et al. [48] showed that the based structural phase is formed by nanodomains characteristics of *P4bm* symmetry with $a^0a^0c^+$ oxygen octahedra tilt. In this case, our ceramics $0 \leq x \leq 0.07$, could have a similar structural phase formed of PNRs since its XRD patterns reveal a rhombohedral *(R3c)* structure without any distortion (Figure 1). The stable phase is a relaxor with coexistence of PNRs with different symmetries *(R3c + P4bm)*. The tetragonal *P4bm* PNRs could be in insufficient amount to be revealed in XRD analysis and not enough to establish any macroscopic effect at low temperature. During heating, the initial phase *R3c* PNRs could be initiated to undergo a phase transition into *P4bm* PNRs where their amount increases with temperature so that the materials transit totally into a tetragonal *(P4bm)* phase. This transition was also proven by Koch et al. using the activation energy obtained from the dielectric conductivity for this temperature range [49]. In addition, they showed that the activation energies are temperature-dependent relating it to phase transition and/or coexistence of rhombohedral and tetragonal phases.

The relaxor behavior revealed in this system ($0 \leq x \leq 0.07$) is mostly due to the thermal evolution of discrete *R3c* PNRs leading to ferroelectric – relaxor phase transition. This evolution transforms the *R3c* PNRs to *P4bm* PNRs, resulting in interaction and coherence of dipoles within PNRs domains. This thermal evolution extends over a large temperature range, hence a frequency-dependent shoulder (broad peak) is measurable in the dielectric properties.

The evolution of the maximum relaxor temperature (T_{MR}) as a function of x is shown in Figure 6. It can be observed that the T_{MR} exponentially decreases with x concentration reaching a constant value for x = 0.05 and 0.07. This is accompanied by a decrease of the ferroelectric transition temperature which is related to the ferroelectric – relaxor transition.

As a result, the CT concentration decreases sharply the T_{F-R}. The maximum of relaxor behavior (T_{MR}) appears and shifts to lower temperatures, i.e. 380 K (107 °C) for x = 0.00 to 320 K (47 °C) for x = 0.05 and 0.07. Therefore, the CT substitution facilitates the ferroelectric – relaxor transition while initiating the relaxor phase at low temperature (even below room temperature). This kind of results is observed for $x \geq 0.15$, where a typical behavior for relaxor ferroelectric is obtained at low temperature (T=231 K (-42°C) for x=0.20) [35]. This can be explained by the fact that the ferroelectric macrodomains of NBT is divided into polar micro and/or nano-domains leading to the decreases of T_{MR} when the CT concentration increases.

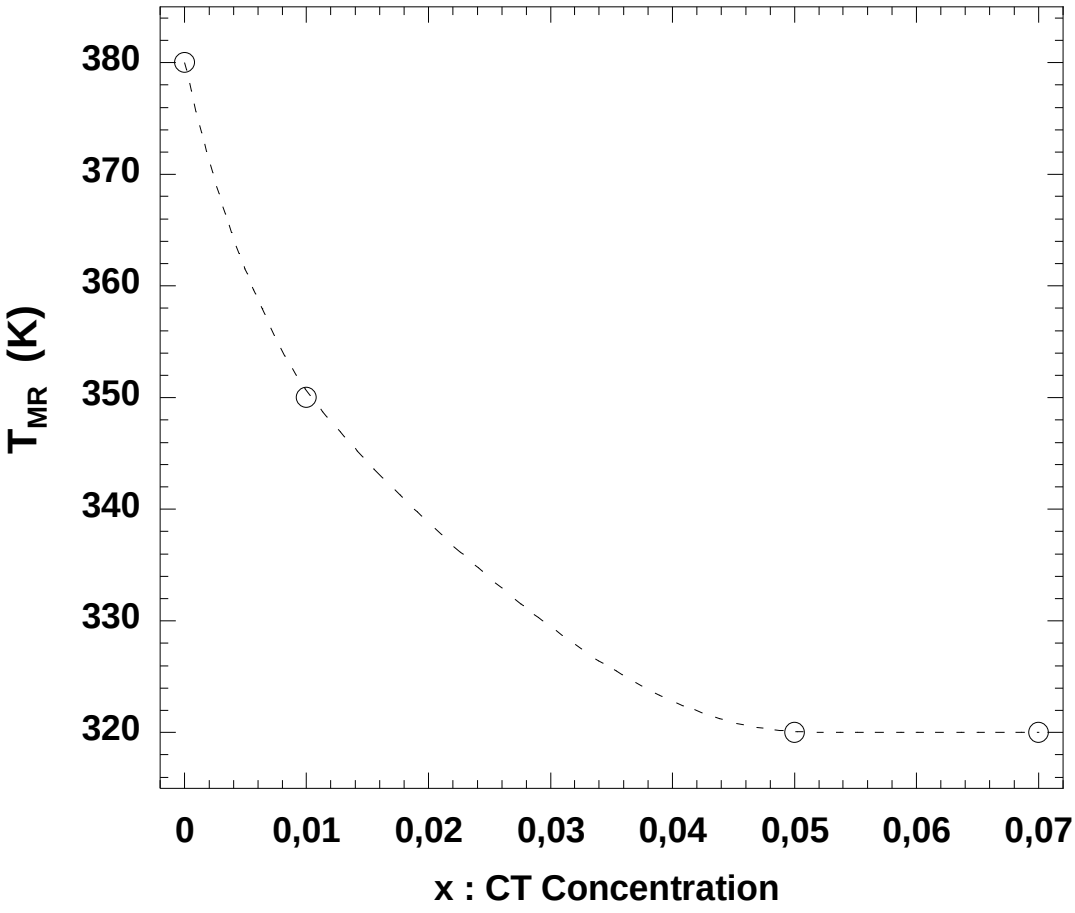

Figure 6: Variation of the maximum relaxor temperature (T_{MR}) as a function of x

4. Conclusion

In this paper, we have investigated and quantified the relaxor properties of lead-free (1-x)$N_{0.5}B_{0.5}TiO_3$ – x$CaTiO_3$ ((1-x)NBT – xCT) system with $0.00 \leq x \leq 0.07$. The structural and vibrational properties of materials synthesized by a solid-state reaction and sintering were studied. The XRD analysis revealed a pure monophasic perovskite with rhombohedral *(R3c)* phase at room temperature for all compositions. Raman spectroscopy showed a local disorder without modifying the symmetry of all solid solutions, which proves the stability of the rhombohedral *(R3c)* structure for low CT concentration. Dielectric measurements at low temperature showed that the compositions with low concentration of CT exhibit dielectric properties similar to the pure NBT i.e. the same dispersive behavior. It revealed a frequency-dependent anomaly as a shoulder, corresponding to the ferroelectric – relaxor transition (T_{F-R}). This anomaly is correlated to the coexistence of polar nanoregions (PNRs) with different symmetries *(R3c + P4bm)* and their thermal evolution. This phenomenon was highlighted by introducing a new concept of dispersion order which was proven to be a valuable parameter in attempting to quantify the relaxor behavior and the determination of

its maximum temperature (T_{MR}).

5. Acknowledgments

This work was supported by the French Ministry of Higher Education and Research, the Nanosciences Department of Université de Bourgogne, and the Lebanese American University.

References

[1] G. O. Jones, P. A. Thomas, Investigation of the structure and phase transitions in the novel A-site substituted distorted perovskite compound Na0.5Bi0.5TiO3, Acta Crystallographica Section B 58 (2002) 168–178.

[2] B. N. Rao, R. Datta, S. S. Chandrashekaran, D. K. Mishra, V. Sathe, A. Senyshyn, R. Ranjan, Local structural disorder and its influence on the average global structure and polar properties in Na0.5Bi0.5TiO3, Phys. Rev. B 88 (2013) 224103.

[3] E. Aksel, J. S. Forrester, J. C. Nino, K. Page, D. P. Shoemaker, J. L. Jones, Local atomic structure deviation from average structure of Na0.5Bi0.5TiO3: Combined x-ray and neutron total scattering study, Physical Review B 87 (2013) 104113.

[4] L. E. Cross, Relaxor ferroelectrics, Ferroelectrics 76 (1987) 241–267.

[5] J. Ravez, A. Simon, Some Solid State Chemistry Aspects of Lead-Free Relaxor Ferroelectrics, Journal of Solid State Chemistry 162 (2001) 260–265.

[6] I. W. Chen, Structural origin of relaxor ferroelectrics—revisited, Journal of Physics and Chemistry of Solids 61 (2000) 197–208.

[7] G. O. Jones, P. A. Thomas, The tetragonal phase of Na0.5Bi0.5TiO3 - a new variant of the perovskite structure, Acta Crystallographica Section B 56 (2000) 426–430.

[8] E. Aksel, J. S. Forrester, J. L. Jones, P. A. Thomas, K. Page, M. R. Suchomel, Monoclinic crystal structure of polycrystalline Na0.5Bi0.5TiO3, Applied Physics Letters 98 (2011) 152901–3.

[9] B. N. Rao, R. Ranjan, Electric-field-driven monoclinic-to-rhombohedral transformation in Na1/2Bi1/2TiO3, Physical Review B 86 (2012) 134103.

[10] L. Luo, W. Ge, J. Li, D. Viehland, C. Farley, R. Bodnar, Q. Zhang, H. Luo, Raman spectroscopic study of Na1/2Bi1/2TiO3-x%BaTiO3 single crystals as a function of temperature and composition, Journal of Applied Physics 109 (2011) 113507–6.

[11] B. K. Barick, K. K. Mishraull, A. K. Arora, R. N. P. Choudhary, K. P. Dillip, Impedance and Raman spectroscopic studies of (Na0.5Bi0.5)TiO3, Journal of Physics D: Applied Physics 44 (2011) 355402.

[12] V. Dorcet, G. Trolliard, P. Boullay, Reinvestigation of Phase Transitions in Na0.5Bi0.5TiO3 by TEM. Part I: First Order Rhombohedral to Orthorhombic Phase Transition, Chemistry of Materials 20 (2008) 5061–5073.

[13] S. B. Vakhrushev, V. A. Isupov, B. E. Kvyatkovsky, N. M. Okuneva, I. P. Pronin, G. A. Smolensky, P. P. Syrnikov, Phase transitions and soft modes in sodium bismuth titanate, Ferroelectrics 63 (1985) 153–160.

[14] D. Rout, K.-S. Moon, S.-J. L. Kang, I. W. Kim, Dielectric and Raman scattering studies of phase transitions in the (100 - x)Na0.5Bi0.5TiO3–xSrTiO3 system, Journal of Applied Physics 108 (2010) 084102–7.

[15] G. Trolliard, V. Dorcet, Reinvestigation of Phase Transitions in Na0.5Bi0.5TiO3 by TEM. Part II: Second Order Orthorhombic to Tetragonal Phase Transition, Chemistry of Materials 20 (2008) 5074–5082.

[16] E. Aksel, J. S. Forrester, B. Kowalski, J. L. Jones, P. A. Thomas, Phase transition sequence in sodium bismuth titanate observed using high-resolution x-ray diffraction, Applied Physics Letters 99 (2011) 222901–3.

[17] K. Sakata, Y. Masuda, Ferroelectric and antiferroelectric properties of (Na0.5Bi0.5)TiO3-SrTiO3 solid solution ceramics, Ferroelectrics 7 (1974) 347–349.
[18] J. Suchanicz, I. P. Mercurio, P. Marchet, T. V. Kruzina, Axial Pressure Influence on Dielectric and Ferroelectric Properties of Na0.5Bi0.5TiO3 Ceramic, physica status solidi (b) 225 (2001) 459–466.
[19] J.-R. Gomah-Pettry, S. Sai, P. Marchet, J.-P. Mercurio, Sodium-bismuth titanate based lead-free ferroelectric materials, Journal of the European Ceramic Society 24 (2004) 1165–1169.
[20] R. Selvamani, G. Singh, V. Sathe, V. S. Tiwari, P. K. Gupta, Dielectric, structural and Raman studies on (Na0.5Bi0.5TiO3)(1 - x)(BiCrO3)x ceramic, J Phys Condens Matter 23 (2011) 055901.
[21] W. Jo, S. Schaab, E. Sapper, L. A. Schmitt, H.-J. Kleebe, A. J. Bell, J. Rödelull, On the phase identity and its thermal evolution of lead free (Bi1/2Na1/2)TiO3-6mol% BaTiO3, Journal of Applied Physics 110 (2011) 074106.
[22] E. Sapper, S. Schaab, W. Jo, T. Granzow, J. Rödel, Influence of electric fields on the depolarization temperature of Mn-doped (1-x)Bi1/2Na1/2TiO3-xBaTiO3, Journal of Applied Physics 111 (2012) 014105.
[23] F. Craciun, C. Galassi, R. Birjega, Electric-field-induced and spontaneous relaxor-ferroelectric phase transitions in (Na1/2Bi1/2)1−xBaxTiO3, Journal of Applied Physics 112 (2012) 124106.
[24] W. Bai, D. Chen, P. Zheng, J. Xi, Y. Zhou, B. Shen, J. Zhai, Z. Ji, NaNbO3 templates-induced phase evolution and enhancement of electromechanical properties in <00l> grain oriented lead-free BNT-based piezoelectric materials, Journal of the European Ceramic Society 37 (2017) 2591–2604.
[25] C. S. Tu, I. G. Siny, V. H. Schmidt, Sequence of dielectric anomalies and high-temperature relaxation behavior in Na1/2Bi1/2TiO3, Physical Review B 49 (1994) 11550–11559.
[26] V. Isupov, Ferroelectric Na0.5Bi0.5TiO3 and K0.5Bi0.5TiO3 Perovskites and Their Solid Solutions, Ferroelectrics 315 (2005) 123–147.
[27] S.-E. Park, K. S. Hong, Variations of Structure and Dielectric Properties on Substituting A-site Cations for Sr2+ in (Na1/2Bi1/2)TiO3, Journal of Materials Research 12 (1997) 2152–2157.
[28] J. Suchanicz, The effect of a.c. and d.c. electric field on the dielectric properties of Na0.5Bi0.5TiO3 ceramic, Condensed Matter Physics 2 (1999) 649–654.
[29] I. P. Aleksandrova, Y. N. Ivanov, A. A. Sukhovskiĭ, S. B. Vakhrushev, 23Na NMR in the relaxor ferroelectric Na1/2Bi1/2TiO3, Physics of the Solid State 48 (2006) 1120–1123.
[30] Y. Watanabe, Y. Hiruma, H. Nagata, T. Takenaka, Phase transition temperatures and electrical properties of divalent ions (Ca2+, Sr2+ and Ba2+) substituted (Bi1/2Na1/2)TiO3 ceramics, Ceramics International 34 (2008) 761–764.
[31] T. Karthik, A. Saket, Monoclinic Cc -phase stabilization in magnetically diluted lead free Na1/2Bi1/2TiO3 —Evolution of spin glass like behavior with enhanced ferroelectric and dielectric properties, Materials Research Express 2 (2015) 096301.
[32] J. R. Gomah-Pettry, A. N. Salak, P. Marchet, V. M. Ferreira, J. P. Mercurio, Ferroelectric relaxor behaviour of Na0.5Bi0.5TiO3–SrTiO3 ceramics, physica status solidi (b) 241 (2004) 1949–1956, null.
[33] W. Krauss, D. S. tz, F. A. Mautner, A. Feteira, K. Reichmann, Piezoelectric properties and phase transition temperatures of the solid solution of (1 - x)(Bi0.5Na0.5)TiO3-xSrTiO3, Journal of the European Ceramic Society 30 (2010) 1827–1832.
[34] J.-K. Lee, K. S. Hong, C. K. Kim, S.-E. Park, Phase transitions and dielectric properties in A-site ion substituted (Na1/2Bi1/2)TiO3 ceramics (A=Pb and Sr), Journal of Applied Physics 91 (2002) 4538–4542.
[35] R. Roukos, N. Zaiter, D. Chaumont, Relaxor behaviour and phase transition of perovskite ferroelectrics-type complex oxides (1–x)Na0.5Bi0.5TiO3–xCaTiO3 system, Journal of Advanced Ceramics 7 (2018) 124–142.
[36] W. Bai, D. Chen, P. Zheng, B. Shen, J. Zhai, Z. Ji, Composition- and temperature-driven phase transition characteristics and associated electromechanical properties in Bi0.5Na0.5TiO3-based lead-free ceramics, Dalton Transactions 45 (2016) 8573–8586.
[37] R. Ranjan, V. Kothai, R. Garg, A. Agrawal, A. Senyshyn, H. Boysen, Degenerate rhombohedral and orthorhombic states in Ca-substituted Na0.5Bi0.5TiO3, Applied Physics Letters 95 (2009) 042904.

[38] R. Rajeev, G. Rohini, A. Anupriya, S. Anatoliy, B. Hans, Phases in the (1 − x)Na0.5Bi0.5TiO3 – (x)CaTiO3 system, Journal of Physics: Condensed Matter 22 (2010) 075901.
[39] E. Birks, M. Dunce, R. I. et al, Structure and dielectric properties of Na0.5Bi0.5TiO3-CaTiO3 solid solutions, Journal of Applied Physics 119 (2016) 074102.
[40] J. Kreisel, A. Glazer, G. J. et al., An x-ray diffraction and Raman spectroscopy investigation of A-site substituted perovskite compounds: the (Na1- xKx)0.5Bi0.5TiO3 (0le xle1) solid solution, Journal of Physics: Condensed Matter 12 (2000) 3267.
[41] R. Roukos, Transitions de phases dans des oxydes complexes de structure pérovskite : cas du système (1-x)Na0,5Bi0,5TiO3 - xCaTiO3, null (2015).
[42] X. G. Tang, K. H. Chew, H. L. W. Chan, Diffuse phase transition and dielectric tunability of Ba(ZryTi1-y)O3 relaxor ferroelectric ceramics, Acta Materialia 52 (2004) 5177–5183.
[43] K. Wang, A. Hussain, W. Jo, J. Rödel, Temperature-Dependent Properties of (Bi1/2Na1/2)TiO3–(Bi1/2K1/2)TiO3–SrTiO3 Lead-Free Piezoceramics, Journal of the American Ceramic Society 95 (2012) 2241–2247.
[44] X. Wang, H. L.-W. Chan, C. loong Choy, Piezoelectric and dielectric properties of CeO2-added (Bi0.5Na0.5)0.94Ba0.06TiO3 lead-free ceramics, Solid State Communications 125 (2003) 395–399.
[45] B.-J. Chu, D.-R. Chen, G.-R. Li, Q.-R. Yin, Electrical properties of Na1/2Bi1/2TiO3-BaTiO3 ceramics, Journal of the European Ceramic Society 22 (2002) 2115–2121.
[46] Y. Yuan, C. J. Zhao, X. H. Zhou, B. Tang, S. R. Zhang, High-temperature stable dielectrics in Mn-modified (1-x) Bi0.5Na0.5TiO3-xCaTiO3 ceramics, Journal of Electroceramics 25 (2010) 212–217.
[47] Y. Yuan, E. Z. Li, B. Li, B. Tang, X. H. Zhou, Effects of Ca and Mn Additions on the Microstructure and Dielectric Properties of (Bi0.5Na0.5)TiO3 Ceramics, Journal of Electronic Materials 40 (2011) 2234–2239.
[48] C. Ma, X. Tan, E. Dul'kin, M. Roth, Domain structure-dielectric property relationship in lead-free (1−x)(Bi1/2Na1/2)TiO3-xBaTiO3 ceramics, Journal of Applied Physics 108 (2010) 104105.
[49] L. Koch, S. Steiner, K.-C. Meyer, I.-T. Seo, K. Albe, T. Frömling, Ionic conductivity of acceptor doped sodium bismuth titanate: influence of dopants, phase transitions and defect associates, Journal of Materials Chemistry C 5 (35) (2017) 8958–8965.